Acta Crystallographica Section F
Structural Biology and Crystallization Communications
ISSN 1744-3091

Precipitation diagram and optimization of crystallization conditions at low ionic strength for deglycosylated dye-decolorizing peroxidase from a basidiomycete

Shinya Saijo,[a] Takao Sato,[a] Nobuo Tanaka,[a] Atsushi Ichiyanagi,[b] Yasushi Sugano[b] and Makoto Shoda[a]*

[a]Graduate School of Bioscience and Biotechnology, Tokyo Institute of Technology, 4259-B-10 Nagatsuta, Midori-ku, Yokohama 226-8501, Japan, and [b]Chemical Resources Laboratory, Tokyo Institute of Technology, 4259-R1-29 Nagatsuta, Midori-ku, Yokohama 226-8503, Japan

Correspondence e-mail: mshoda@res.titech.ac.jp

Received 18 February 2005
Accepted 21 June 2005
Online 8 July 2005

The growth of suitably sized protein crystals is essential for protein structure determination by X-ray crystallography. In general, crystals are grown using a trial-and-error method. However, these methods have been modified with the advent of microlitre dispensing-robot technology and of protocols that rapidly screen for crystal nucleation conditions. The use of one such automatic dispenser for mixing protein drops (1.3–2.0 µl in volume) of known concentration and pH with precipitating solutions (ejecting 2.0 µl droplets) containing salt is described here. The results of the experiments are relevant to a crystallization approach based on a two-step procedure: screening for the crystal nucleation step employing robotics followed by optimization of the crystallization conditions using incomplete factorial experimental design. Large crystals have successfully been obtained using quantities as small as 3.52 mg protein.

1. Introduction

An automatic dispenser for screening protein crystallization conditions was pioneered by Chayen *et al.* (1990) and subsequently developed as a robot capable of performing on a microlitre volume scale and used to carry out a large number of microbatch-under-oil crystallization experiments (Chayen *et al.*, 1992, 1994; Chayen, 1996, 1997, 1998, 1999; Baldock *et al.*, 1996; D'Arcy *et al.*, 1996; Lorber & Giegé, 1996). The use of dispensing robots for crystallization experiments may be an efficient means to minimize sample loss, especially during initial screening. Experiments using the nanolitre dispensing system (Sulzenbacher *et al.*, 2002) were performed with several commercially available screening kits (Jancarik & Kim, 1991). However, no matter how small the amount of protein sample the robots may dispense, it remains difficult to predict and to optimize the conditions obtained from preliminary screening based on only a standard trial-and-error procedure. In cases where the initial crystallization screening trials have failed, the use of dispensing robots may be helpful in constructing conditions that could lead to crystal growth. Presently, only a few protocols are available to rapidly screen for nucleation (and growth) conditions. Thus, we attempted to quantify protein/precipitation concentrations, temperature and pH values by applying incomplete factorial approaches (Carter & Carter, 1979). Previously, Carter & Yin (1994) scored crystal growth by deriving the ratios of the smallest dimension to the largest one using a microscopic reticule. In place of such an approach, we scored crystal growth by the width of the crystals, which is correlated to their diffraction intensities, since the illuminated crystal volume can be estimated from the thickness of crystal and the X-ray beam size.

In this study, we performed crystallization experiments using a novel glycosylated protein dye-decolorizing peroxidase (DyP) which is secreted by the decolorizing fungus *Thanatephorus cucumeris* Dec 1 and plays an important role in the degradation of anthraquinone dyes. Deglycosylation was performed in order to reduce intermolecular steric repulsions caused by the three N-linked glycans on the surface of the protein, which hamper crystal growth. In our previous work, we obtained hexagonal DyP crystals under conditions of high ionic strength containing 0.89 *M* $(NH_4)_2SO_4$ and 0.92 *M* NaCl pH 4.2 (Sato *et al.*, 2004). A dimer was found in the asymmetric unit. Crystals of poor quality were obtained at the pI of DyP, presumably owing to the appearance of two conformational isomers (faulty

conformations), which was detected by IEF (unpublished data). These faulty conformations were a consequence of the partial negative charges on residues such as Glu and Asp at this pH. In order to obtain crystals that diffract to higher resolution, we performed crystallizations using solutions containing NaCl at low concentrations, PEG 8000 and MES buffer at neutral pH. We selected the two latter components of the crystallization solutions based on the previous finding that deglycosylated DyP exhibits enzymatic activity and is stable for more than 26 d either in MES buffer at pH 6 or in 45% methanol (unpublished data). Liquid-handling robots are essential for accurate dispensing of microlitre volumes of precipitants with high viscosity such as PEG 8000. Here, we used the Hydra II Plus One system (Matrix Technologies Corporation, NH, USA) to set up sitting-drop plates on the microlitre scale (Walter *et al.*, 2003) in screening for crystallization conditions of DyP based on its precipitant solubility curve.

2. Materials and methods

2.1. Construction of precipitation curves

The deglycosylated DyP (48 kDa) was produced as described in Sato *et al.* (2004). DyP was identified as a single band by SDS–PAGE and was thus of a suitable grade for crystallization trials. The protein concentration of DyP was estimated from the molar absorption coefficient (36 565 M^{-1} cm^{-1}) at 280 nm (Pace *et al.*, 1995). Since the lead crystallization condition was initially unknown, a grid-screening system consisting of 96 vapour-diffusion experiments was employed to determine the initial precipitate conditions. Preparation of the precipitant solutions for initial screening was performed in Greiner 96 deep-well plates (Greiner Bio-One, Inc., Tokyo, Japan) and the compositions of the precipitants were varied as follows: 10.0–46.5%(*w*/*v*) PEG 8000 at 3.0%(*w*/*v*) intervals and 200–400 m*M* NaCl at 15 m*M* intervals in 0.1 *M* MES buffer pH 6.0. In order to draw the precipitation diagram, crystallization trials were performed on a 96-well IntelliPlate (Art Robbins Enterprises, CA, USA) using the Hydra system with 96 stainless-steel syringes to dispense the precipitant solutions aspirated from the Greiner deep-well plates and with an additional non-contact single-channel microsolenoid dispenser to pipette DyP into a 0.5 ml Eppendorf tube. The DyP concentration was gradually changed from 6.29 to 9.19 mg ml^{-1} by transferring 1.3–2 µl of the DyP solution with the single-channel dispenser at 0.1 µl intervals with respect to every line on the 96-well IntelliPlate.

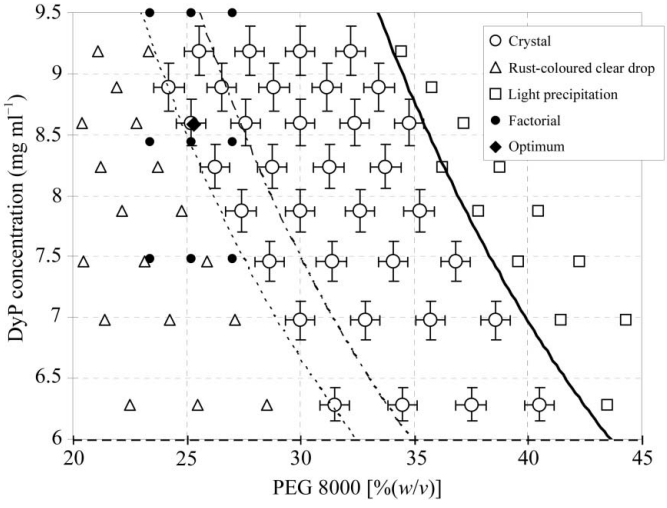

Figure 1
Precipitation diagrams of deglycosylated DyP at pH 6.0 and 277 K. The precipitation curve, plotted using a full line, was defined by the first signs of light precipitation formation (squares) and then by crystal formation (circles), excluding the rust-coloured clear-drop zones (triangles). Error bars of the *x* and *y* axes were estimated from the dispensing accuracy, with standard errors in the PEG 8000 and protein concentrations of 0.18 and 0.07, respectively. The grey-framed rectangle indicates the concentration intervals (filled circles) chosen for optimization with an incomplete factorial design as the nucleation (and growth) zone. The largest single crystal obtained is denoted by a filled diamond. The boundary line between the crystal and clear-drop zones of DyP with PEG 8000 indicates the nucleation concentration curve and is plotted using a dashed line. The middle of the three lines, plotted using a dotted and dashed line, is defined as the boundary between crystal and spherulite formation.

The dispensing accuracies of the single-channel dispenser and the 96-syringe assembly were evaluated by dispensing Color Index Reactive Blue 5 (Nippon Kayaku Co., Tokyo, Japan). The volumes of the dispensed solutions were calculated from the concentrations of the dye, which was measured using a Multiskan JX plate ELISA reader (Thermo Labsystems, Yokohama, Japan). This dyestuff used has a molar absorption coefficient of 7590.0 M^{-1} cm^{-1} at 630 nm.

The accuracy of the single-channel dispenser was 1.18% CV [the ratio of the average (1.70 µl) and the standard deviation (20.0 nl)] for 1.3 µl and 0.87% CV (average 0.92 µl and standard deviation 8.0 nl) for 2 µl DyP, while that of the 96-syringe assembly was 0.05% CV (average 2 µl and standard deviation 0.001 µl, CV 0.05%) for the setting value of 2 µl precipitant solution.

2.2. Optimization of crystallization conditions

A matrix consisting of 15 conditions based on an incomplete factorial approach was designed for optimizing the crystallization conditions. Using the *Xtalgrow Screen Design* software (http://jmr.xtal.pitt.edu/xtalgrow/), entries in the designed 15 × 4 matrix were interpreted as 0, centre, −1, low end and +1, high end of the variable range. The droplets were viewed every other day under a microscope at magnifications of 50–80×. The crystallization conditions under which spherulites and amorphous precipitate formed and small crystals appeared were placed at the centre of a matrix of 15 conditions. Subsequently, the input parameters were set for this matrix as follows: pH values of 5.5, 5.8 and 6.1, temperatures of 277, 280 and 283 K, PEG 8000 concentrations of 23.4, 25.2 and 27.0%(*w*/*v*) and DyP concentrations of 7.48, 8.44 and 9.50 mg ml^{-1}. Optimization experiments were carried out using the dispensing-robot system with the vapour-diffusion method. Microscopic measurements were also performed to score the crystals according to their widths. Statistical methods as regression analysis, analysis of variance (ANOVA) and response-surface modelling were applied in order to quantify the dependence on the four factors of the crystallization conditions (Carter & Carter, 1979; Yin & Carter, 1996). All statistical calculations were carried out using the *SPSS* software (SPSS Japan Inc., Tokyo, Japan).

2.3. Cryocooling and data collection

Prior to flash-freezing, the DyP crystals were briefly soaked in a cryoprotectant solution containing 20%(*v*/*v*) glycerol, 35%(*w*/*v*) PEG 8000, 0.6 *M* NaCl and 0.1 *M* MES buffer pH 6.0. All data were collected at 95 K using an ADSC Quantum 315 detector (Area Detector Systems Corporation, CA, USA) on the BL5 beamline at the Photon Factory (Tsukuba, Japan). Data were processed at the 1.35 Å resolution limit and reduced using the *CrystalClear* software (Rigaku/MSC, TA, USA).

3. Results and discussion

3.1. Precipitation diagram

The location of the nucleation zone, where a protein can form nuclei, is indicated on the precipitation diagram shown in Fig. 1. In this case particulates precipitated and spherulites (Fig. 2*a*) and small crystals were obtained from conditions belonging to this zone after 1 d. After 3 d, large crystals (Fig. 2*b*) were formed just above the zone boundary separating the clear-drop and crystal zones. The precipitate curve is denoted on the diagram as the boundary between crystal and light-precipitate formation. It is fitted to an exponential curve (Gaucher *et al.*, 1997) using

$$[\text{Protein}] = 41.433 \exp -0.0441[\text{Precipitant}], \quad (1)$$

where [Protein] and [Precipitant] are the concentrations of DyP protein (mg ml^{-1}) and PEG 8000 [%(*w*/*v*)].

A nucleation concentration (crystal solubility) curve has also been described as an approximated curve at the boundary line between the clear drop and the crystal. It is defined by

$$[\text{Protein}] = 29.898 \exp -0.0489[\text{Precipitant}]. \quad (2)$$

The protein and precipitant concentrations of the nucleation concentration (crystal solubility) curve are 27 and 10% lower than those of the precipitation curve, respectively. However, these concentrations may vary depending on the type of protein and on the crystallization conditions. Once a precipitation diagram has been plotted for a novel protein, then the precipitation curve can help to provide the maximum concentrations for crystallization. Taking only conditions along a nucleation concentration (crystal solubility) curve dependent on (2) may be a direct and useful tool for deriving and optimizing the appropriate crystallization conditions under which crystals of suitable width may be obtained.

3.2. Crystal optimization

For crystallization, it is essential that the protein concentration be close or just below the crystal solubility curve in the form of (2). It is also practical to estimate the optimum point in the incomplete factorial design with matrices of 15 experiments designed to explore the factor space identified from the precipitate and the crystal solubility curves. Only 0.92 mg of DyP was consumed in replicate experiments that required 0.46 mg per 15 runs. The experimental data can be fitted to a linear model by regression analysis and ANOVA.

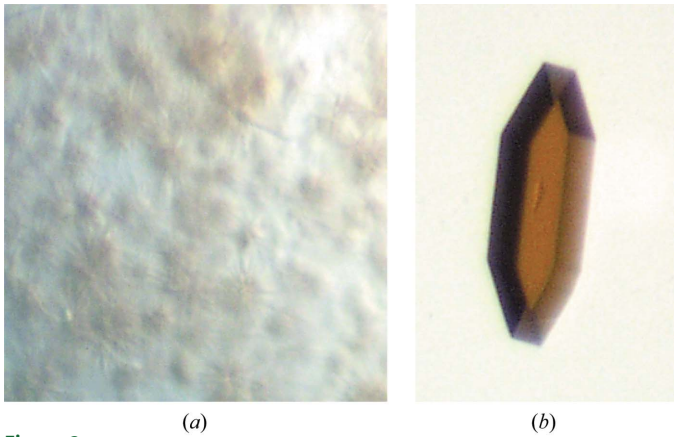

(*a*) (*b*)

Figure 2
(*a*) Spherulites on the surface of the drop, which were observed before crystal formation, under a microscope at full-range magnification of 110×. (*b*) DyP crystal obtained using the sitting-drop vapour-diffusion method. The rust-coloured crystal is in the form of a hexagonal prism and belongs to a monoclinic system.

Table 1
Crystal data of deglycosylated DyP and diffraction statistics.

Values in parentheses are for the highest resolution shell.

Crystal of deglycosylated DyP	Low ionic strength	High ionic strength†
Protein concentration (mg ml^{-1})	8.6	15
Precipitant	25.3%(*w*/*v*) PEG 8000	0.89 *M* $(NH_4)_2SO_4$
Buffer	0.1 *M* MES	0.1 *M* sodium citrate
pH	6.2	4.2
Additive NaCl (*M*)	0.23	0.92
Temperature (K)	278.5	283
Degree of supersaturation‡	2.7	5.5
Crystal system	Monoclinic	Hexagonal
Space group	$P2_1$	$P6_522$
Unit-cell parameters		
a (Å)	47.1	136.15
b (Å)	95.9	136.15
c (Å)	50.3	363.46
β (°)	104.1	
V_M (Å^3 Da^{-1})	2.30	4.98
Solvent content (%)	46.62	75.75
Asymmetric unit	Monomer	Dimer
Wavelength (Å)	1.0000	
Resolution (Å)	1.35 (1.40–1.35)	2.96 (3.10–2.96)
$I/\sigma(I)$	6.8 (2.0)	
Total observations	375635	
Unique reflections	183670	
Completeness (%)	98.1 (97.2)	
R_{merge}§ (%)	4.7 (27.0)	

† Previous work reported by Sato *et al.* (2004). ‡ The degree of supersaturation is defined as σ_s = (protein concentration − solubility)/solubility. § $R_{merge} = \sum_{hi} |\langle I(h)\rangle - I(h)_i| / \sum_h \sum_i I(h)_i$, where $I(h)$ is the intensity of reflection h, $\sum_h$ is the sum of over all reflections and $\sum_i$ is the sum of all i measurements of reflection h.

Subsequently, using the response-surface method, the optimum crystallization condition was then estimated from the model as follows: 8.6 mg ml^{-1} DyP, 25.3%(*w*/*v*) PEG 8000 and 278.5 K (pH 6.2). It implies that the point *C* where high-quality crystals occur is located just above the crystal solubility curve of the form given in (2). Reproducibility was also demonstrated, as evidenced by a significant convergence between the replicated experiments achieved within a residual error of 6%. Our experiment clearly indicates that the automatic method combining dispensing-robot technology and stochastic analysis can yield better crystals than those obtained from conventional manual crystallization methods. Finally, while the precipitation diagram can exhibit a synergetic effect of PEG 8000 and protein concentrations on crystallization behaviour, it can also anticipate the multiplier effect of pH and temperature. These four parameters were sampled in the incomplete factorial design and then fitted to a linear model by regression analysis and ANOVA.

3.3. Diffraction data

As shown in Fig. 2(*b*), a deglycosylated DyP crystal was obtained in a drop volume of 4.0 µl, the maximum size being 0.27 × 0.075 × 0.063 mm, which was observed under a microscope at full-range magnification of 110×. It diffracted to a resolution of 1.35 Å, which was higher than that previously reported for a crystal obtained at high ionic strength (Sato *et al.*, 2004). The space group could be identified as $P2_1$. The crystals had unit-cell parameters a = 47.1, b = 95.9, c = 50.3 Å, β = 104.1° and contained one DyP molecule per asymmetric unit. The protein exists as a monomer in solution, which determined by gel chromatography and by DLS (Sato *et al.*, 2004). The unit-cell volume was 2.2140 × 10^5 Å^3. Based on the MW of the monomer being 48 kDa, a solvent content of 46.62% and a V_M value of 2.30 Å^3 Da^{-1} were obtained, which are within the range assigned to a typical protein crystal by Matthews (1968). Table 1 provides the data-collection details.

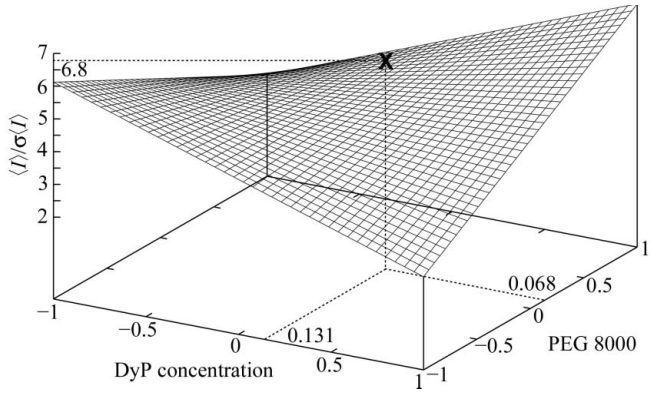

Figure 3
Response-surface plot of the measured crystal quality *versus* protein and precipitate concentrations. The average $\langle I\rangle/\sigma\langle I\rangle$ is dependent on DyP and PEG 8000 concentrations. The surface plot was shown in the variable range between −1 [7.48 mg ml^{-1} DyP, 23.4%(*w*/*v*) PEG 8000] and +1 [9.50 mg ml^{-1} DyP, 27.0%(*w*/*v*) PEG 8000]. The maximum of $\langle I\rangle/\sigma\langle I\rangle$ is of 6.8 and represents the optimum point on the surface, indicated by *X*. The figure was prepared using *GNUPLOT* (http://www.gnuplot.info).

Based on ANOVA, a response-surface plot of the average ratio of observed intensity of crystals *versus* protein and PEG concentrations is shown in Fig. 3. A maximum $\langle I\rangle/\sigma\langle I\rangle$ of 6.8 was predicted as the stationary point (*X*) with optimal conditions of 0.131 and 0.068. It corresponds to 8.6 mg ml^{-1} DyP and 28.14% PEG 8000 at a high pH of 6.1 and a low temperature of 278.7 K on the nucleation-curve plot.

4. Conclusions

When it was essential to know the crystallization condition and required great quantities of protein sample to produce the precipitation diagram, protein crystallographers used to avoid constructing the diagrams as much as possible. With the advent of microlitre-drop dispensers, there is no longer any reason for the diagrams not to be established through practical protein crystallography. Particularly when working with high-viscosity precipitants, an automatic dispensing system is suitable for construction of the diagram and for optimization of the crystallization conditions. High precision is crucial in dispensing small volumes to separate clear-drop from light-precipitate zones. It is possible that these results will provide a future direction and a strategic thrust for making more rational choices with respect to protein crystallization. Therefore, by employing robot technology, the crystal-screening method is expected to have a potential for wide use at present and in the near future.

We are grateful to SCRUM Inc. for permitting us to use the Hydra II Plus One system. Special thanks are due to Messrs Yoshiyuki Maeno and Yusuke Osawa, SCRUM Inc. as well as Masayasu Tsuchikura, Altair Corporation for their help. This research was undertaken with the approval of the Photon Factory Advisory Committee, Japan. The authors wish to express their sincere thanks to the staff at the Photon Factory for the help during data collection. This work was partly supported by a Grant from the 21st Century COE Program and a Grant-in-Aid for Scientific Research (C) from the Japanese Ministry of Education, Culture, Sports, Science and Technology.

References

Baldock, P., Mills, V. & Shaw Stewart, P. D. (1996). *J. Cryst. Growth*, **168**, 170–174.
Carter, C. W. Jr & Carter, C. W. (1979). *J. Biol. Chem.* **254**, 12219–12223.
Carter, C. W. Jr & Yin, Y. (1994). *Acta Cryst.* D**50**, 572–590.
Chayen, N. E. (1996). *Protein Eng.* **9**, 927–929.
Chayen, N. E. (1997). *Structure*, **5**, 1269–1274.
Chayen, N. E. (1998). *Acta Cryst.* D**54**, 8–15.
Chayen, N. E. (1999). *J. Cryst. Growth*, **196**, 434–441.
Chayen, N. E., Shaw Stewart, P. D. & Baldock, P. (1994). *Acta Cryst.* D**50**, 456–458.
Chayen, N. E., Shaw Stewart, P. D. & Blow, D. M. (1992). *J. Cryst. Growth*, **122**, 176–180.
Chayen, N. E., Shaw Stewart, P. D., Maeder, D. L. & Blow, D. M. (1990). *J. Appl. Cryst.* **23**, 297–302.
D'Arcy, A., Elmore, C., Stihle, M. & Johnson, J. E. (1996). *J. Cryst. Growth*, **168**, 175–180.
Jancarik, J. & Kim, S.-H. (1991). *J. Appl. Cryst.* **24**, 409–411
Lorber, B. & Giegé, R. (1996). *J. Cryst. Growth*, **168**, 204–215.
Matthews, B. W. (1968). *J. Mol. Biol.* **33**, 491–497.
Gaucher, J. F., Riès-Kautt, M., Reiss-Husson, F. & Ducruix, A. (1997). *FEBS Lett.* **401**, 113–116.
Pace, C. N., Vajdos, F., Fee, L., Grimsley, G. & Gray, T. (1995). *Protein Sci.* **4**, 2411–2423.
Sato, T., Hara, S., Matsui, T., Sazaki, G., Saijo, S., Ganbe, T., Tanaka, N., Sugano, Y. & Shoda, M. (2004). *Acta Cryst.* D**60**, 149–152.
Sulzenbacher, G. *et al.* (2002). *Acta Cryst.* D**58**, 2109–2115
Walter, T. S., Diprose, J., Brown, J., Pickford, M., Owens, R. J., Stuart, D. I. & Harlos, K. (2003). *J. Appl. Cryst.* **36**, 308–314.
Yin, Y. & Carter, C. W. Jr (1996). *Nucleic Acids Res.* **24**, 1279–1286.